2018

Transient Lattice Deformations of Crystals Studied by Means of Ultrafast Time-Resolved X-Ray and Electron Diffraction

Runze Li

Kyle Sundqvist

Jie Chen

H. E. Elsayed-Ali
Old Dominion University, helsayed@odu.edu

Jie Zhang

See next page for additional authors

Original Publication Citation

Li, R., Sundqvist, K., Jie, C., Elsayed-Ali, H. E., Jie, Z., & Rentzepis, P. M. (2018). Transient lattice deformations of crystals studied by means of ultrafast time-resolved x-ray and electron diffraction. *Structural Dynamics, 5*(4), 044501. doi:10.1063/1.5029970

Transient lattice deformations of crystals studied by means of ultrafast time-resolved x-ray and electron diffraction

Runze Li, Kyle Sundqvist, Jie Chen, H. E. Elsayed-Ali, Jie Zhang, and Peter M. Rentzepis

Citation: Structural Dynamics **5**, 044501 (2018); doi: 10.1063/1.5029970
View online: https://doi.org/10.1063/1.5029970
View Table of Contents: http://aca.scitation.org/toc/sdy/5/4
Published by the American Institute of Physics

Transient lattice deformations of crystals studied by means of ultrafast time-resolved x-ray and electron diffraction

Runze Li,[1,a)] Kyle Sundqvist,[2] Jie Chen,[3] H. E. Elsayed-Ali,[4] Jie Zhang,[3] and Peter M. Rentzepis[1,b)]
[1]*Department of Electrical and Computer Engineering, Texas A&M University, College Station, Texas 77843, USA*
[2]*Department of Physics, San Diego State University, San Diego, California 92182, USA*
[3]*Center for Ultrafast Science and Technology, Key Laboratory for Laser Plasmas (Ministry of Education), School of Physics and Astronomy, Collaborative Innovation Center of IFSA (CICIFSA), Shanghai Jiao Tong University, Shanghai 200240, China*
[4]*Department of Electrical and Computer Engineering, Old Dominion University, Norfolk, Virginia 23529, USA*

(Received 17 March 2018; accepted 12 June 2018; published online 27 June 2018)

Ultrafast lattice deformation of tens to hundreds of nanometer thick metallic crystals, after femtosecond laser excitation, was measured directly using 8.04 keV subpicosecond x-ray and 59 keV femtosecond electron pulses. Coherent phonons were generated in both single crystal and polycrystalline films. Lattice compression was observed within the first few picoseconds after laser irradiation in single crystal aluminum, which was attributed to the generation of a blast force and the propagation of elastic waves. The different time scales of lattice heating for tens and hundreds nanometer thick films are clearly distinguished by electron and x-ray pulse diffraction. The electron and lattice heating due to ultrafast deposition of photon energy was simulated using the two-temperature model and the results agreed with experimental observations. This study demonstrates that the combination of two complementary ultrafast time-resolved methods, ultrafast x-ray, and electron diffraction will provide a panoramic picture of the transient structural changes in crystals. [https://doi.org/10.1063/1.5029970]

I. INTRODUCTION

Probing dynamics with a sub-angstrom structural and femtosecond temporal resolution is the key to track the pathways and intermediate states in chemical reactions and understand the functions of materials at a fundamental level. Because the lattice vibrational time is typically around 100 fs, there are no mechanical or electronic means that are sufficiently fast to capture such ultrafast processes. However, following the time-resolved studies of pulsed-photon-induced reactions in the early 1950s,[1] the pump-probe method was developed, which demonstrated for the first time, a picosecond temporal resolution for chemical reactions.[2,3] Several years later, after the introduction of femtosecond laser pulses,[4] tracing the dissociation and formation of chemical bonds, which occur within a femtosecond time interval, became possible.[5] Among the various pump/probe combinations, optical pump/optical probe,[6,7] optical pump/electron probe,[8–12] and optical pump/x-ray probe[13–16] are the three most widely used experimental means. Purely optical methods, such as transient spectroscopy[17] or transient reflectivity measurement,[18] usually provide information on the relaxation of the electron systems after laser excitation, while the dynamics concerning the structural changes are obtained indirectly through

[a)]Email: Runze@tamu.edu
[b)]Email: prentzepis@tamu.edu

theoretical modeling. Ultrafast time-resolved diffraction methods that employ x-ray[19–21] and/or electron pulses,[22–27] however, provide direct information on the structural dynamics as they interact directly with the atoms and/or inner shell electrons. The femtosecond and picosecond x-ray pulses can be generated by large national facilities, free electron lasers,[28–30] and small compact systems that are based on laser-plasma interaction[31] and are suitable for university size laboratories. The femtosecond electron pulses are usually generated by photo-electron guns and accelerated by table-top DC electric fields[32,33] or RF fields[27,34,35] to tens of keV or a few MeV, respectively. Time-resolved electron diffraction can record higher-order Bragg diffractions and enable the observation of diffuse scatterings;[36] however, the presence of tens of kV/m transient electric fields on the metallic or semiconductor sample[37–39] may make the interpretation of electron diffraction data difficult.[40,41] Therefore, additional treatments to the diffraction patterns or estimation of the field strengths are necessary.[38,42,43] On the other side, as charged particles, electron pulses are suitable for diagnosing fast-evolving plasmas or warm dense matter that involves transient electro-magnetic fields.[44–47] Meanwhile, x-ray pulses are insensitive to transient electric fields and their diffraction signals are solely related to lattice structure. The limited yield and the flux instability of hard x-ray photons generated by the laser-plasma sources, however, make it rather difficult to obtain a high signal-to-noise ratio for diffraction intensities. In addition, the optical skin depth of metals is typically on the order of a few nanometers, which is close to the penetration depth of the keV electron beam, while much shorter than that of the x-ray penetration depth into the bulk of the sample. Therefore, for tens of nanometer thick samples, where homogeneous laser excitation is expected, it is more accurate and convenient to use electron pulses, while for hundreds nanometer thick samples, it is more appropriate to use x-ray pulses that probe not only the surface, but also the bulk that is heated due to the laser energy deposited onto the surface layer and transferred to the interior of the crystals. Therefore, using results from both time-resolved ultrafast electron and x-ray diffraction, which are two highly complementary methods, may provide a more detailed description of the transient structural dynamics of crystals, than either method can provide alone.[48]

In this paper, the transient structural changes of aluminum crystals, illuminated with femtosecond laser pulses, were recorded in real time with the combination of x-ray and electron probes. In both experiments, the aluminum crystals are heated to a similar equilibrium temperature. The ultrafast heating of the electron and lattice subsystems was simulated using the two-temperature model (TTM), which agrees with experimental observations. The oscillation periods of crystals with different thicknesses are measured by both transmission and reflection diffractions, which agreed with the standing wave assumption.

II. EXPERIMENTAL METHOD

The methods used in our experiments are demonstrated in Fig. 1. The ultrafast time-resolved x-ray diffraction experiments were performed on a table-top system that generates hard x-ray pulses through laser/plasma interaction.[49] The 800 nm, 100 fs, 100 mJ laser pulse emitted from a 10 Hz Ti:sapphire laser was split into two parts. 80% of the laser energy is focused onto a 0.5 mm diameter copper wire that is continuously moving in a vacuum chamber to generate 8.04 keV Cu Kα sub-picosecond x-ray pluses. The upper limit of the x-ray pulse duration is estimated to be 0.6 ps.[50] The x-ray pulses were collimated by a 200 μm slit and impinged onto a 150 nm thick Al (111) single crystal in a reflecting diffraction configuration with a Bragg diffraction angle of 18.9°. The remaining 20% of the laser energy is frequency doubled to 400 nm and used to excite the sample. Before focusing onto the sample, the 400 nm excitation laser pulse is directed to a linear translation stage that precisely controls the arrival time between the probe x-ray pulses and the pump laser pulses. The Al (111) single crystal used in our experiments was grown on Mica substrate at a base temperature of 150 °C.

The ultrafast time-resolved electron diffraction experiments were performed on a table-top system that is capable of delivering sub-picosecond, 59 keV, electron pulses.[38] The 800 nm, 70 fs, 1 mJ laser pulse emitted by a 1 kHz Ti:sapphire laser system is split into two parts by a beam splitter. 40% of the laser energy is frequency tripled to 266.7 nm and directed to the silver

photocathode, using a back illumination, to generate electrons, which were accelerated to 59 keV by a DC electrical field and focused by a magnetic lens onto the sample to form a transmission diffraction configuration in the ultra-high vacuum chamber ($<1 \times 10^{-9}$ Torr). The remaining 60% of the laser energy, which is attenuated and used to excite the polycrystalline aluminum sample, is directed to a translation stage that can control precisely the arrival time between the pump laser pulse and the probe electron pulse at the sample. The temporal-resolution of the ultrafast time-resolved electron diffraction system is estimated to be 0.5 ps. The 10–20 nm thick polycrystalline Al films used in this study were obtained as follows: First, they were deposited onto freshly cleaved NaCl single crystal surfaces, then immersed into deionized water, and subsequently transferred to transmission electron microscope (TEM) grids as freestanding films.

The x-ray diffraction patterns were recorded directly by a 2D x-ray charge-coupled device (CCD) camera, while the electron diffraction patterns were converted into optical signals on a phosphor screen, amplified by an image intensifier and eventually recorded by a 2D optical CCD. Because the sample used in the time-resolved x-ray diffraction experiments is ∼10 times thicker than the ones used in ultrafast electron diffraction experiments, the pump laser fluences used for such experiments are about 10 times higher than in the electron diffraction experiments, in order for the crystals to be heated to the same equilibrium temperatures in both experiments. In both the electron and x-ray experiments, the pump laser fluencies are below the damage threshold of aluminum. The time-dependent changes in the diffraction peaks were analyzed and correlated with transient atomic motions. According to the first-order Bragg diffraction equation, $2d \sin\theta = \lambda$, where d is the lattice plane distance, θ is the Bragg angle, and λ is the wavelength of probing electrons of x-ray photons, one can obtain the following relation: $\Delta d/d = -\Delta\theta/\tan\theta$, which directly connects the relative change of the lattice plane distance with the change of diffraction angles, obtained from the experimentally recorded diffraction patterns. For keV or MeV electron diffraction, because the diffraction angle is typically small (less than 1°), the small angle approximation may be applied and therefore one could use $\Delta d/d = -\Delta\theta/\tan\theta \approx -\Delta\theta/\theta$.

III. RESULTS AND DISCUSSION

A. Transient structural changes of single crystal and polycrystalline aluminum films

The transient structural changes of the 150 nm thick Al (111) single crystal after illumination with 400 nm femtosecond laser pulses were probed by 8.04 keV sub-picosecond x-ray pulses. The diffraction peak shift, which represents the relative changes in the lattice plane distance, and the broadening of the diffraction line width as a function of time are shown in Fig. 2. The data show that the relative change of the lattice plane distance is negative during the first few picoseconds after laser excitation, which reveals that contraction takes place and the lattice plane distance becomes shorter. Following the contraction, damping oscillations of the lattice plane were developed, accompanying a lattice plane expansion. The new equilibrium position of the lattice plane distance was formed ∼120 ps after illumination with the femtosecond pulse(s). The initial contraction of the lattice plane distance is due to the formation of a compressive wave that was initiated on the surface layer of the crystal as a result of a blast force.[51–54] Because the x-ray pulse penetrates and probes the entire 150 nm thick crystal, the contraction formed within the top few lattice layers accounts for less than 10% of the overall diffraction signal. Therefore, the contraction observed during the first few picoseconds is small, ∼8%, compared with the observed expansion of the lattice. Such contraction was also observed previously in Au single crystals.[55] We are aware that transient electric fields will build up on the crystal surface upon femtosecond laser excitation. Our previous studies have shown that the maximum transient electric field, at ∼150 μm above the aluminum sample surface, is on the order of tens kV/m for a few mJ/cm^2 pump fluencies.[56] Although the pump fluence used for the 150 nm single crystal sample is higher, the transient electric field strength may not be higher than those observed in aluminum plasmas generated by femtosecond laser excitation.[46] This is because that, the electrons that escaped at earlier times tend to suppress further emission of

electrons due to the space charge effects (Coulomb repulsion), which is well documented in photoemission studies,[57] thus limit the strength of transient electric fields. Such effects are also observed in transient electric field measurements on GaN.[47] Moreover, the single crystal aluminum film used in the x-ray experiments is at atmospheric pressure, which further reduces the transient electric field strength and as a grounded conductor, the electric fields are also prohibited from penetrating into the bulk of aluminum. Therefore, the contraction observed in the first few picoseconds is not due to transient surface electric fields. After the contraction stage, the laser energy initially deposited within the skin depth of the crystal propagates through the bulk and heats the entire crystal through electron-phonon and phonon-phonon interaction. The elevated crystal temperature is reflected by the increased shift of the diffraction line peaks and the increased strain is indicated by the broadening of diffraction line width. The increase in the lattice plane distance is accompanied by several damping oscillations, which indicate that coherent phonons were generated. Such lattice damping oscillations have been observed in a number of time-resolved diffraction studies.[20,58,59] These oscillations represent the vibration of the lattice and the damping is accompanied by the dissipation of energy into the surroundings or the conversion of kinetic energy into heat. The mechanism of acoustic oscillations may be explained theoretically using the thermal strain-stress model or the Fermi-Pasta-Ulam anharmonic chain model.[60–62] The oscillation is generally simplified by considering it as the formation of a one-dimensional standing wave between the surface and crystal substrate. Therefore, the oscillation period, T, may be calculated using the sound velocity of the crystal: $T = 2L/v$, where $L = 150$ nm is the film thickness and the sound velocity in solid aluminum $v = 6420$ m/s.[63] The oscillation period was calculated to be ∼47 ps, which is in agreement with our experimentally observed value of ∼41 ps. The diffraction peak shift remains unchanged after the damping oscillation for ∼180 ps, which is the longest delay time in our experiments.

The transient structural changes measured by sub-picosecond x-ray pulse experiments were also compared with those obtained through ultrafast time-resolved electron diffraction experiments. To avoid the effects of transient electric fields, on the shift of the electron diffraction peak,[38] a transmission diffraction configuration was employed in the ultrafast electron diffraction experiments. Polycrystalline aluminum films of three different thicknesses, 10 nm, 15 nm, and 20 nm, were interrogated by 59 keV, sub-picosecond electron pulses. The relative changes of the (311) lattice plane distance for those films are shown in Fig. 3 and the theoretical and experimental periods versus crystal thickness are listed and compared in Table I. It is worth mentioning that because the 10 nm thick film contains only a few layers of lattice, it might not be a continuous polycrystalline film and is most likely built up with flat connected islands. In the transmission electron diffraction configuration, the electron beam may not be strictly perpendicular to the aluminum sample surface because the probe electrons travel spirally after the magnetic lens and the freestanding aluminum films have curvatures. It is clear that the lattice expansion was observed immediately after the laser excitation at a fluence of ∼2.1 mJ/cm^2. The maximum expansion of the lattice plane distance is achieved within a few picoseconds after laser excitation and the new equilibrium state is established around tens of picoseconds, which is much shorter than the equilibrium time observed in x-ray diffraction experiments presented above. This is because the film thickness in electron diffraction experiments is comparable or close to the penetration depth of laser pulses. Therefore, the entire crystal is expected to be heated evenly within the first few picoseconds and contributes homogeneously to the electron diffraction pattern. In the x-ray diffraction case, however, the excitation laser energy is also absorbed within the skin depth, while the x-ray pulse probes the entire crystal, which in this case is about twenty times longer than the skin depth. Therefore, a much longer time is required to transfer the heat to the entire probing depth of the sample which travels with sound velocity. This process requires tens or hundreds of picoseconds depending on the thickness of the crystal.

B. Electron and lattice heating described by the two-temperature model (TTM)

Upon femtosecond laser irradiation, the photon energy is initially deposited into the free electrons within the skin depth of the 150 nm thick Al (111) crystal within the duration of the

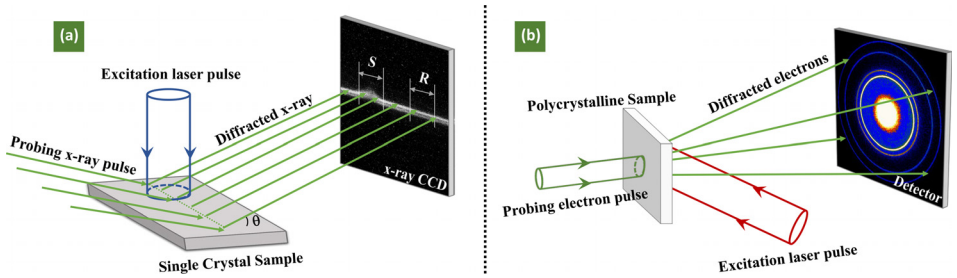

FIG. 1. Schematic diagram of the ultrafast time-resolved x-ray and electron diffraction methods. (a) The diffraction from a single crystal sample investigated by sub-picosecond x-ray pulses. The x-ray diffraction signal originated from the laser excitation area of the Al (111) crystal was marked "S" on the detector, while "R" denoted the reference without laser irradiation. (b) The electron diffraction for polycrystalline Al sample investigated by femtosecond electron pulses. The angle between the front-illumination laser and back-probing electron beams is ∼10° to minimize the geometric mismatch and improve temporal resolution.

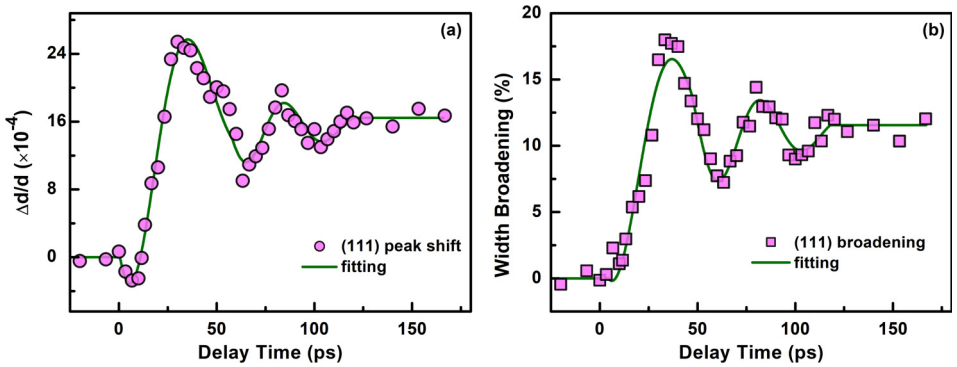

FIG. 2. Time-dependent relative change of (a) diffraction peak position and (b) diffraction line width boarding of a 150 nm thick single crystal Al (111) film interrogated by sub-picosecond x-ray pulses in a reflection diffraction configuration. The excitation laser fluence is 18.5 mJ/cm^2.

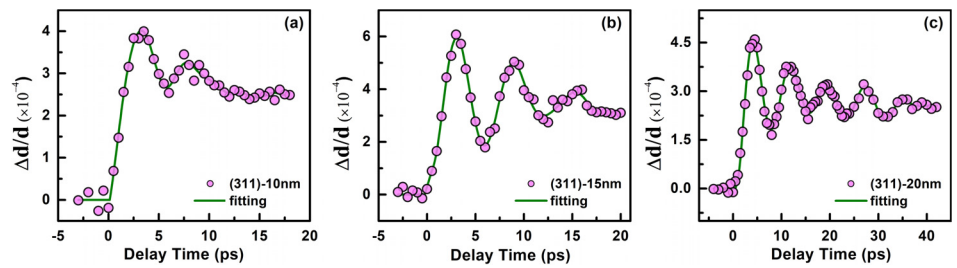

FIG. 3. Time-dependent relative change of the (311) lattice plane distance of (a) 10 nm, (b) 15 nm, and (c) 20 nm thick polycrystalline aluminum freestanding films interrogated by femtosecond electron pulses in a transmission diffraction configuration. The laser pump fluence is 2.1 mJ/cm^2 on each sample.

TABLE I. Oscillation periods of Al samples with three different thicknesses. The theoretical period was calculated using the one-dimensional standing wave model.

Sample thickness (nm)	10 ± 3	15 ± 3	20 ± 3
Theoretical oscillation period (ps)	3.1 ± 0.9	4.7 ± 0.9	6.2 ± 0.9
Experimental oscillation period (ps)	3.8	6.0	6.4
Sample thickness inferred from experimental period (nm)	12	19	21

femtosecond laser pulse. Tens or hundreds of femtoseconds after the initial stage, the entire electron system reaches equilibrium through electron-electron interaction. Because the electron-electron scattering is more efficient than electron-phonon interaction, the electron temperature may reach tens of thousands of Kelvin, while the lattice remains cold, at room temperature, within tens to hundreds of femtoseconds after laser excitation. Subsequently, the heat transport between electrons and lattice occurs by means of electron-phonon interaction. The heat capacity of the electrons, C_e, is typically orders of magnitude smaller than that of the lattice heat capacity, C_l. The rate of energy exchange between the electron and lattice system is described by the electron-phonon coupling, g, and the temperature equilibration between the electron and lattice subsystems usually takes place within picoseconds through electron-phonon and phonon-phonon interactions. Heat transport within metals illuminated with ultrashort laser pulses is generally described by the well-established two-temperature model, in which the temperature evolution of the electron and lattice subsystems is described by two coupled heat transport equations. Because the area probed by the x-ray or electron pulses is several times smaller than that of the diameter of the laser excitation area, the three-dimensional laser-matter interaction could be reduced to a one-dimensional representation along the sample thickness direction. The electron and lattice heating of the 150 nm aluminum crystal, in this study, may therefore be described by the following two-temperature model (TTM):[9,64,65]

$$C_e \frac{\partial}{\partial t} T_e(z,t) = \frac{\partial}{\partial z}\left(\kappa_e \frac{\partial}{\partial z} T_e(z,t)\right) - g[T_e(z,t) - T_L(z,t)] + S(z,t), \tag{1}$$

$$C_L \frac{\partial}{\partial t} T_L(z,t) = g[T_e(z,t) - T_L(z,t)], \tag{2}$$

where $T_e(z,t)$ and $T_L(z,t)$ are the electron and lattice temperatures at the depth z under the aluminum sample surface at a certain time t, respectively. The excitation laser pulse is described by $S(z,t)$ which has a Gaussian profile and k_e is the electron thermal conductivity. Ballistic electron motion is not considered, in this case, because it contributes insignificantly to the heating of the film. Under low excitation fluences, where the electron temperature may increase by only a few hundreds or thousands Kelvin, it is appropriate to assume that the electron-phonon coupling, g, and the electron heat capacity and thermal conductivity, C_e and k_e, are linearly dependent on the electron temperature or may be simply treated as constants. For electron temperatures that may increase by more than tens of thousands Kelvin, more sophisticated modeling maybe required. There has been a large number of literature papers concerning the application of TTM to time-resolved diffraction studies.[25,66,67] Here, we use the one that is applicable to both low and higher laser excitation fluences[59,68] and it is worthy to note that at lower excitation fluences, Eqs. (3)–(5) reduce to approximately a linear dependence on temperature. In the following simulation, the Drude model is used for electron-electron and electron-phonon scattering; therefore, the electron thermal conductivity (W/mK) is given by:[69–71]

$$\kappa_e = \frac{a_0 T_e}{a_1 T_e^2 + a_2 T_L}, \tag{3}$$

where $a_0 = 1.08 \times 10^{14}$, $a_1 = 5.2 \times 10^6$, and $a_2 = 4.61 \times 10^{11}$. The electron-phonon coupling, g (W/m^3 K), and electron heat capacity, C_e (J/m^3 K) are provided by the fifth-order Padé approximations

$$g = 1 \times 10^{17} \frac{\sum_{n=0}^{5} A_1(n)\left(\frac{T_e}{10^4}\right)^n}{1 + \sum_{n=1}^{5} A_2(n)\left(\frac{T_e}{10^4}\right)^n}, \tag{4}$$

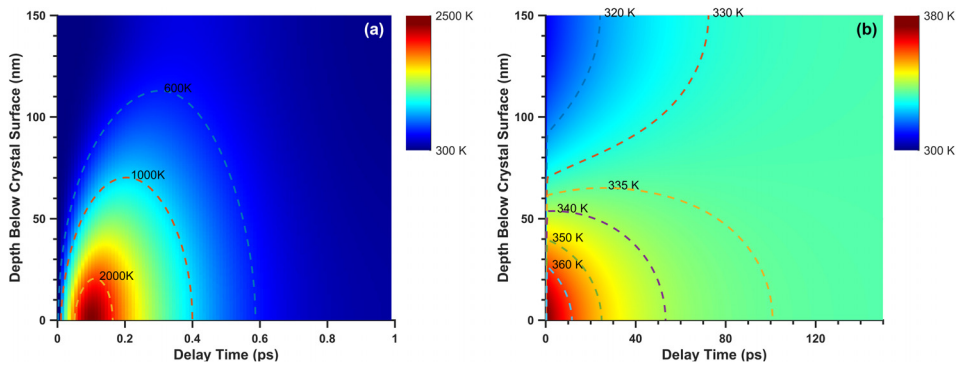

FIG. 4. Two-temperature model simulation of the 150 nm thick aluminum crystal illuminated by 18.5 mJ/cm^2 femtosecond laser pulse. (a) Spatial-temporal distribution of the electron temperature; (b) spatial-temporal distribution of the lattice temperature.

$$C_e = 1 \times 10^5 \frac{\sum_{n=0}^{5} B_1(n)\left(\frac{T_e}{10^4}\right)^n}{1 + \sum_{n=1}^{5} B_2(n)\left(\frac{T_e}{10^4}\right)^n}, \tag{5}$$

where $A_1(0) = 2.4897$, $A_1(1) = -3.5228$, $A_1(2) = 99.2859$, $A_1(3) = -125.4458$, $A_1(4) = 116.2749$, and $A_1(5) = -19.5488$; $A_2(1) = -0.6301$, $A_2(2) = 24.2843$, $A_2(3) = -29.5203$, $A_2(4) = 28.8661$, and $A_2(5) = -4.8065$; $B_1(0) = 0.0348$, $B_1(1) = 5.7659$, $B_1(2) = 51.9519$, $B_1(3) = -16.9218$, $B_1(4) = 121.2319$, and $B_1(5) = -17.4062$; $B_2(1) = 2.0446$, $B_2(2) = 7.087$, $B_2(3) = 3.3556$, $B_2(4) = 2.0852$, and $B_2(5) = -0.3873$.

The spatial-temporal distributions of both electron and lattice temperatures, of the 150 nm thick Al (111) crystal, after femtosecond laser excitation are simulated by the theoretical model discussed above and plotted in Fig. 4. It is found that the highest electron temperature of 2500 K can be reached within 100 fs, which is essentially the pulse width of the femtosecond laser pulse(s) used in our experiments. The thermalization of the electron system within the 150 nm thick Al crystal, occurring in less than 1 ps, is accompanied by the energy transfer from the electron system to the lattice system through electron-phonon coupling. The lattice temperature may reach as high as 380 K within the first few picoseconds, after laser irradiation, and then equilibrate with the bulk of the crystal through thermal diffusion and phonon-phonon interaction. Our numerical simulation suggested that the largest non-equilibrium temperature occurs during the first 30 ps, which agrees with the experimental results shown in Fig. 2 where the lattice expansion kept increasing for the first tens of picoseconds after laser excitation. The thermal equilibrium state of the entire 150 nm crystal may be established within 100 ps. However, it should be noted that because this model describes only the temperature evolution and does not simulate the motion of each individual atom, the lattice oscillations observed in the experiments discussed here are not incorporated in the simulation.

IV. CONCLUSION

Using sub-picosecond 8.04 keV x-ray pulses and 59 keV femtosecond electron pulses as probes, we systematically probed and recorded the transient structural changes of single crystal and polycrystalline aluminum films irradiated with femtosecond laser pulses, respectively. Coherent phonons were generated and observed in aluminum films of different thicknesses, and the experimentally observed oscillation periods agree with the values suggested by one-dimensional standing wave model. Lattice contraction of the single crystal was detected, which indicated the generation of blast force due to the non-equilibrium electron pressure. The different time scales for heating tens and hundreds of nanometer thick metallic lattices are clearly

distinguished by electron and x-ray pulse experiments. The electron and lattice heating processes were numerically simulated using the two-temperature model and the results agree with the experimental observations. The combination of these two methods, in a single experimental frame, has been demonstrated in this study and it provided a powerful means for obtaining detailed information of the transient structural changes in crystals of various thicknesses.

ACKNOWLEDGMENTS

We gratefully acknowledge the partial support of the Welch Foundation (Grant No. 1501928), the Air Force Office of Scientific Research (Grant No. FA9550-18-1-0100), and the Texas A&M University TEES funds. Jie Chen thanks the support of the National Natural Science Foundation of China under Grant Nos. 11574196, 61222509, and 11421064. H. E. Elsayed-Ali acknowledges support of the National Science Foundation Grant No. DMR-170817.

[1]G. Porter, "Flash photolysis and spectroscopy. A new method for the study of free radical reactions," Proc. R. Soc. London, Ser. A **200**(1061), 284–300 (1950).
[2]P. M. Rentzepis, "Direct measurements of radiationless transitions in liquids," Chem. Phys. Lett. **2**(2), 117–120 (1968).
[3]P. M. Rentzepis, "Emission from the lowest singlet and triplet states of azulene," Chem. Phys. Lett. **3**(9), 717–720 (1969).
[4]C. V. Shank and E. P. Ippen, "Subpicosecond kilowatt pulses from a mode-locked cw dye laser," Appl. Phys. Lett. **24**(8), 373–375 (1974).
[5]C. V. Shank, E. P. Ippen, and R. Bersohn, "Time-resolved spectroscopy of hemoglobin and its complexes with subpicosecond optical pulses," Science **193**(4247), 50 (1976).
[6]P. M. Rentzepis, "Advances in picosecond spectroscopy," Science **218**(4578), 1183 (1982).
[7]S. Mukamel, "Multidimensional femtosecond correlation spectroscopies of electronic and vibrational excitations," Annu. Rev. Phys. Chem. **51**(1), 691–729 (2000).
[8]G. Mourou and S. Williamson, "Picosecond electron diffraction," Appl. Phys. Lett. **41**(1), 44–45 (1982).
[9]H. E. Elsayed-Ali, T. B. Norris, M. A. Pessot, and G. A. Mourou, "Time-resolved observation of electron-phonon relaxation in copper," Phys. Rev. Lett. **58**(12), 1212 (1987).
[10]A. A. Ischenko, V. P. Spiridonov, L. Schäfer, and J. D. Ewbank, "The stroboscopic gas electron diffraction method for investigation of time-resolved structural kinetics in photoexcitation processes," J. Mol. Struct. **300**, 115–140 (1993).
[11]J. R. Helliwell and P. M. Rentzepis, *Time-Resolved Diffraction* (Oxford University Press, Oxford, 1997).
[12]V. A. Lobastov, J. D. Ewbank, L. Schäfer, and A. A. Ischenko, "Instrumentation for time-resolved electron diffraction spanning the time domain from microseconds to picoseconds," Rev. Sci. Instrum. **69**(7), 2633–2643 (1998).
[13]T. Anderson, I. V. Tomov, and P. M. Rentzepis, "A high repetition rate, picosecond hard x-ray system, and its application to time-resolved x-ray diffraction," J. Chem. Phys. **99**(2), 869–875 (1993).
[14]C. Rose-Petruck, R. Jimenez, T. Guo, A. Cavalleri, C. W. Siders, F. Rksi, J. A. Squier, B. C. Walker, K. R. Wilson, and C. P. J. Barty, "Picosecond-milliangstrom lattice dynamics measured by ultrafast X-ray diffraction," Nature **398**(6725), 310–312 (1999).
[15]M. Bargheer, N. Zhavoronkov, Y. Gritsai, J. C. Woo, D. S. Kim, M. Woerner, and T. Elsaesser, "Coherent atomic motions in a nanostructure studied by femtosecond X-ray diffraction," Science **306**(5702), 1771 (2004).
[16]G. C. O'Neil, L. Miaja-Avila, Y. I. Joe, B. K. Alpert, M. Balasubramanian, D. M. Sagar, W. Doriese, J. W. Fowler, W. K. Fullagar, N. Chen, G. C. Hilton, R. Jimenez, B. Ravel, C. D. Reintsema, D. R. Schmidt, K. L. Silverman, D. S. Swetz, J. Uhlig, and J. N. Ullom, "Ultrafast time-resolved X-ray absorption spectroscopy of ferrioxalate photolysis with a laser plasma X-ray source and microcalorimeter array," J. Phys. Chem. Lett. **8**(5), 1099–1104 (2017).
[17]J. Chen, T. C. Cesario, and P. M. Rentzepis, "Time resolved spectroscopic studies of methylene blue and phenothiazine derivatives used for bacteria inactivation," Chem. Phys. Lett. **498**(1–3), 81–85 (2010).
[18]C. Guo, G. Rodriguez, A. Lobad, and A. J. Taylor, "Structural phase transition of aluminum induced by electronic excitation," Phys. Rev. Lett. **84**(19), 4493–4496 (2000).
[19]C. W. Siders, A. Cavalleri, K. Sokolowski-Tinten, C. Tóth, T. Guo, M. Kammler, M. H. v. Hoegen, K. R. Wilson, D. v. d. Linde, and C. P. J. Barty, "Detection of nonthermal melting by ultrafast X-ray diffraction," Science **286**(5443), 1340–1342 (1999).
[20]A. Cavalleri, C. Siders, F. Brown, D. Leitner, C. Toth, J. Squier, C. Barty, K. Wilson, K. Sokolowski-Tinten, and M. H. von Hoegen, "Anharmonic lattice dynamics in germanium measured with ultrafast X-ray diffraction," Phys. Rev. Lett. **85**(3), 586 (2000).
[21]H. Ihee, M. Lorenc, T. K. Kim, Q. Y. Kong, M. Cammarata, J. H. Lee, S. Bratos, and M. Wulff, "Ultrafast X-ray diffraction of transient molecular structures in solution," Science **309**(5738), 1223 (2005).
[22]B. J. Siwick, J. R. Dwyer, R. E. Jordan, and R. J. D. Miller, "An atomic-level view of melting using femtosecond electron diffraction," Science **302**(5649), 1382–1385 (2003).
[23]A. H. Zewail and J. M. Thomas, *4D Electron Microscopy: Imaging in Space and Time* (World Scientific, 2009).
[24]P. Musumeci, J. T. Moody, C. M. Scoby, M. S. Gutierrez, M. Westfall, and R. K. Li, "Capturing ultrafast structural evolutions with a single pulse of MeV electrons: Radio frequency streak camera based electron diffraction," J. Appl. Phys. **108**(11), 114513 (2010).
[25]L. Waldecker, R. Bertoni, R. Ernstorfer, and J. Vorberger, "Electron-phonon coupling and energy flow in a simple metal beyond the two-temperature approximation," Phys. Rev. X **6**(2), 021003 (2016).
[26]J. Yang, M. Guehr, T. Vecchione, M. S. Robinson, R. Li, N. Hartmann, X. Shen, R. Coffee, J. Corbett, A. Fry, K. Gaffney, T. Gorkhover, C. Hast, K. Jobe, I. Makasyuk, A. Reid, J. Robinson, S. Vetter, F. Wang, S. Weathersby, C.

Yoneda, M. Centurion, and X. Wang, "Diffractive imaging of a rotational wavepacket in nitrogen molecules with femtosecond megaelectronvolt electron pulses," Nat. Commun. **7**, 11232 (2016).
[27]X. J. Wang, D. Xiang, T. K. Kim, and H. Ihee, "Potential of femtosecond electron diffraction using near-relativistic electrons from a photocathode RF electron gun," J. Korean Phys. Soc. **48**, 390–396 (2006).
[28]C. Bressler and M. Chergui, "Molecular structural dynamics probed by ultrafast X-ray absorption spectroscopy," Annu. Rev. Phys. Chem. **61**, 263–282 (2010).
[29]H. Ihee, M. Wulff, J. Kim, and S.-i Adachi, "Ultrafast X-ray scattering: Structural dynamics from diatomic to protein molecules," Int. Rev. Phys. Chem. **29**(3), 453–520 (2010).
[30]L. X. Chen and X. Zhang, "Photochemical processes revealed by X-ray transient absorption spectroscopy," J. Phys. Chem. Lett. **4**(22), 4000–4013 (2013).
[31]T. Guo, "More power to X-rays: New developments in X-ray spectroscopy," Laser Photonics Rev. **3**(6), 591–622 (2009).
[32]J. Cao, Z. Hao, H. Park, C. Tao, D. Kau, and L. Blaszczyk, "Femtosecond electron diffraction for direct measurement of ultrafast atomic motions," Appl. Phys. Lett. **83**(5), 1044–1046 (2003).
[33]C.-Y. Ruan, Y. Murooka, R. K. Raman, R. A. Murdick, R. J. Worhatch, and A. Pell, "The development and applications of ultrafast electron nanocrystallography," Microsc. Microanal. **15**(4), 323–337 (2009).
[34]S. Tokita, S. Inoue, S. Masuno, M. Hashida, and S. Sakabe, "Single-shot ultrafast electron diffraction with a laser-accelerated sub-MeV electron pulse," Appl. Phys. Lett. **95**(11), 111911 (2009).
[35]R. K. Li and P. Musumeci, "Single-shot MeV transmission electron microscopy with picosecond temporal resolution," Phys. Rev. Appl. **2**(2), 024003 (2014).
[36]P. Zhu, J. Chen, R. Li, L. Chen, J. Cao, Z. Sheng, and J. Zhang, "Laser-induced short-range disorder in aluminum revealed by ultrafast electron diffuse scattering," Appl. Phys. Lett. **103**(23), 231914 (2013).
[37]H. Park and J. M. Zuo, "Direct measurement of transient electric fields induced by ultrafast pulsed laser irradiation of silicon," Appl. Phys. Lett. **94**(25), 251103 (2009).
[38]R.-Z. Li, P. Zhu, L. Chen, J. Chen, J. Cao, Z.-M. Sheng, and J. Zhang, "Simultaneous investigation of ultrafast structural dynamics and transient electric field by sub-picosecond electron pulses," J. Appl. Phys. **115**(18), 183507 (2014).
[39]W. Wendelen, B. Y. Mueller, D. Autrique, B. Rethfeld, and A. Bogaerts, "Space charge corrected electron emission from an aluminum surface under non-equilibrium conditions," J. Appl. Phys. **111**(11), 113110 (2012).
[40]H. Park and J. M. Zuo, "Comment on 'structural preablation dynamics of graphite observed by ultrafast electron crystallography'," Phys. Rev. Lett. **105**(5), 059603 (2010).
[41]F. Carbone, P. Baum, P. Rudolf, and A. H. Zewail, "Carbone *et al*. Reply," Phys. Rev. Lett. **105**(5), 059604 (2010).
[42]R. K. Raman, Z. Tao, T.-R. Han, and C.-Y. Ruan, "Ultrafast imaging of photoelectron packets generated from graphite surface," Appl. Phys. Lett. **95**(18), 181108 (2009).
[43]Z. Tao, H. Zhang, P. M. Duxbury, M. Berz, and C.-Y. Ruan, "Space charge effects in ultrafast electron diffraction and imaging," J. Appl. Phys. **111**(4), 044316 (2012).
[44]M. Centurion, P. Reckenthaeler, S. A. Trushin, F. Krausz, and E. E. Fill, "Picosecond electron deflectometry of optical-field ionized plasmas," Nat. Photonics **2**(5), 315–318 (2008).
[45]J. Li, X. Wang, Z. Chen, J. Zhou, S. S. Mao, and J. Cao, "Real-time probing of ultrafast residual charge dynamics," Appl. Phys. Lett. **98**(1), 011501 (2011).
[46]L. Chen, R. Li, J. Chen, P. Zhu, F. Liu, J. Cao, Z. Sheng, and J. Zhang, "Mapping transient electric fields with picosecond electron bunches," Proc. Natl. Acad. Sci. U. S. A. **112**(47), 14479–14483 (2015).
[47]R. Li, P. Zhu, J. Chen, J. Cao, P. M. Rentzepis, and J. Zhang, "Carrier emission of n-type gallium nitride illuminated by femtosecond laser pulses," J. Appl. Phys. **120**(23), 233107 (2016).
[48]J. Chen and P. M. Rentzepis, "Subpicosecond and sub-angstrom time and space studies by means of light, X-ray, and electron interaction with matter," J. Phys. Chem. Lett. **5**(1), 225–232 (2014).
[49]J. Chen, H. Zhang, I. V. Tomov, and P. M. Rentzepis, "Laser induced transient structures in a 150 nm gold crystal," J. Chin. Chem. Soc. **54**(6), 1619–1628 (2007).
[50]I. V. Tomov, J. Chen, X. Ding, and P. M. Rentzepis, "Efficient focusing of hard X-rays generated by femtosecond laser driven plasma," Chem. Phys. Lett. **389**(4–6), 363–366 (2004).
[51]Y. Gan and J. K. Chen, "Thermomechanical wave propagation in gold films induced by ultrashort laser pulses," Mech. Mater. **42**(4), 491–501 (2010).
[52]J. K. Chen, J. E. Beraun, and C. L. Tham, "Ultrafast thermoelasticity for short-pulse laser heating," Int. J. Eng. Sci. **42**(8–9), 793–807 (2004).
[53]J. K. Chen, J. E. Beraun, L. E. Grimes, and D. Y. Tzou, "Short-time thermal effects on thermomechanical response caused by pulsed lasers," J. Thermophys. Heat Transfer **17**(1), 35–42 (2003).
[54]C. Thomsen, H. T. Grahn, H. J. Maris, and J. Tauc, "Surface generation and detection of phonons by picosecond light pulses," Phys. Rev. B **34**(6), 4129–4138 (1986).
[55]J. Chen, W.-K. Chen, and P. M. Rentzepis, "Blast wave and contraction in Au(111) thin film induced by femtosecond laser pulses. A time resolved x-ray diffraction study," J. Appl. Phys. **109**(11), 113522 (2011).
[56]R.-Z. Li, P. Zhu, L. Chen, T. Xu, J. Chen, J. Cao, Z.-M. Sheng, and J. Zhang, "Investigation of transient surface electric field induced by femtosecond laser irradiation of aluminum," New J. Phys. **16**(10), 103013 (2014).
[57]T. Srinivasan-Rao, J. Fischer, and T. Tsang, "Photoemission studies on metals using picosecond ultraviolet laser pulses," J. Appl. Phys. **69**(5), 3291–3296 (1991).
[58]S. Nie, X. Wang, H. Park, R. Clinite, and J. Cao, "Measurement of the electronic Grüneisen constant using femtosecond electron diffraction," Phys. Rev. Lett. **96**(2), 025901 (2006).
[59]J. Chen, W.-K. Chen, J. Tang, and P. M. Rentzepis, "Time-resolved structural dynamics of thin metal films heated with femtosecond optical pulses," Proc. Natl. Acad. Sci. U.S.A. **108**(47), 18887–18892 (2011).
[60]H. Park, X. Wang, S. Nie, R. Clinite, and J. Cao, "Mechanism of coherent acoustic phonon generation under nonequilibrium conditions," Phys. Rev. B **72**(10), 100301 (2005).
[61]P. Yu, J. Tang, and S.-H. Lin, "Photoinduced structural dynamics in laser-heated nanomaterials of various shapes and sizes," J. Phys. Chem. C **112**(44), 17133–17137 (2008).

[62]J. Tang, "Coherent phonon excitation and linear thermal expansion in structural dynamics and ultrafast electron diffraction of laser-heated metals," J. Chem. Phys. **128**(16), 164702 (2008).
[63]*CRC Handbook of Chemistry and Physics*, edited by D. R. Lide, 82nd ed. (Chemical Rubber Company, Boca Raton, FL, 2001-2002).
[64]M. I. Kaganov, I. M. Lifshitz, and L. V. Tanatarov, "Relaxation between electrons and the crystalline lattice," Sov. Phys. - JETP **4**(2), 173–178 (1957).
[65]S. I. Anisimov, B. L. Kapeliovich, and T. L. Perel'man, "Electron emission from metal surfaces exposed to ultrashort laser pulses," Sov. Phys. - JETP **39**(2), 375–377 (1974).
[66]D. Schick, A. Bojahr, M. Herzog, R. Shayduk, C. von Korff Schmising, and M. Bargheer, "Udkm1Dsim—A simulation toolkit for 1D ultrafast dynamics in condensed matter," Comput. Phys. Commun. **185**(2), 651–660 (2014).
[67]Z. Lin and L. V. Zhigilei, "Time-resolved diffraction profiles and atomic dynamics in short-pulse laser-induced structural transformations: Molecular dynamics study," Phys. Rev. B **73**(18), 184113 (2006).
[68]R. Li, O. A. Ashour, J. Chen, H. E. Elsayed-Ali, and P. M. Rentzepis, "Femtosecond laser induced structural dynamics and melting of Cu (111) single crystal. An ultrafast time-resolved x-ray diffraction study," J. Appl. Phys. **121**(5), 055102 (2017).
[69]N. W. Ashcroft and N. D. Mermin, *Solid State Physics* (Holt, Rinehart and Winston, New York, 1976).
[70]X. Y. Wang, D. M. Riffe, Y. S. Lee, and M. C. Downer, "Time-resolved electron-temperature measurement in a highly excited gold target using femtosecond thermionic emission," Phys. Rev. B **50**(11), 8016–8019 (1994).
[71]T. Q. Qiu and C. L. Tien, "Femtosecond laser heating of multi-layer metals—I. Analysis," Int. J. Heat Mass Transfer **37**(17), 2789–2797 (1994).